Computing the parameter sensitivities of outdoor sound propagation in a random environment

Chris Pettit[a] and Keith Wilson[b]

[a]U.S. Naval Academy, Aerospace Engineering Dept., 590 Holloway Rd., MS 11-B, Annapolis, MD 21402, USA
[b]U.S. Army Cold Regions Research and Engineering Laboratory, 72 Lyme Road, Hanover, 03755-1290, USA
petitcl@usna.edu

Computational forecasts of near-ground sound levels are compromised by uncertainty and discretization errors in the atmosphere and terrain representations, and by simplified or incorrect physics. For an incompletely known environment, a model's predictive power cannot be assessed without first quantifying its sensitivity throughout the parameter space. Knowledge of these sensitivities throughout the spatial domain also is essential for effectively investing data-gathering resources to support sound propagation forecasts. Sensitivity analysis therefore is central to raising the relevance of computational acoustics in practical applications. These considerations should motivate practitioners to adopt a consistent framework for sensitivity and uncertainty analyses. Topics to be discussed include: (1) standard uncertainty taxonomies in computational mechanics, (2) why uncertainty about a parameter should be distinguished from sensitivity of a model to that parameter, (3) sources of uncertainty in the near-ground acoustics, (4) a sampling-based sensitivity analysis framework that facilitates estimating typical and extreme values of sensitivities at each point in the spatial domain (i.e., full-field sensitivities), (5) factors to be aware of when applying sensitivity analysis to forecasts of near-ground sound propagation, and (6) ways of examining sensitivity estimates to facilitate insight.

1 Sensitivity analysis and uncertainty quantification

1.1 Defining the context

Predictions of near-ground sound propagation are compromised by statistical uncertainty and model errors in how the atmosphere and terrain are characterized. High quality physical and numerical representations are available, but imprecise knowledge of the heterogeneous propagation environment impedes attempts to achieve spatial and temporal accuracy in sound field predictions [27]. Embleton [5] summarizes many of these environmental factors, which include (i) the topography and acoustic impedance of the ground or lower boundary of the propagation domain; (ii) the interaction of the wind and radiative exchanges with this surface, which alters the velocity and thermal gradients in the atmospheric surface layer (ASL); and (iii) spatio-temporal variability in atmospheric turbulence. We study full-field sensitivity analysis of near-ground sound propagation throughout the model parameter space, and we summarize a recent framework for computing these sensitivities. The concepts and method presented here can support efforts to define propagation environments so as to ensure high confidence in the predicted sound fields, primarily by promoting the effective use of measurements to support predictions and by providing insight into how limited knowledge compromises predictions.

To bridge the gap between making predictions and justifying confidence in those predictions, the challenge of accounting for the multiple sources of uncertainty described above and their interactions must be addressed. This concern is common to all disciplines that involve the use of complex predictive models, so the field of verification and validation (V&V) of computational mechanics models is evolving to help bridge this gap. Organized efforts to codify V&V concepts and methods include, among others, a guide by the American Institute of Aeronautics and Astronautics [1] for computational fluid dynamics and the more recently published guide for V&V in computational solid mechanics [21].

These documents cite uncertainty quantification (UQ) as a crucial step in the larger problem of verifying and validating predictive models. UQ is too broad to be encapsulated here, so we limit its definition to the process of constructing probabilistic models for forcing functions and system parameters, and transforming these models through a network of computational mechanics models to predict the distribution of a response process. Models will be called deterministic when they do not depend directly on the recognition of uncertainty. Non-probabilistic or generalized probabilistic methods, which commonly involve the introduction of fuzzy or non-additive measures, are not considered; see Ben-Haim [2] and Nikolaidis, et al. [13] for extensive introductions. Assessing deterministic model validity, i.e., physical fidelity, also is not addressed.

1.2 Local, global, and full-field sensitivity analyses

Sensitivity analysis (SA) of a computational model is restricted here to the organized assessment of changes in a model's output due to changes in the parameters. UQ of any complex, multiple parameter model ought to begin with SA to reveal the parameters that can induce the most imprecision and randomness in the response. Doing so helps to determine the relative accuracies required in measurements and probabilistic parameter models.

The most direct SA is to compute through analysis or finite differences how variations in the neighborhood of an baseline parameter values influence an output of interest; this *local SA* [19]. A parallel but distinct concern, especially when SA is used to support UQ, is how to estimate efficiently the range of sensitivities throughout the feasible portion of the multidimensional parameter space; this is *global SA* [19]. The difference is important when a model exhibits substantial variations in its parameter sensitivities, i.e., nonlinear sensitivities, as various neighborhoods in the parameter space are interrogated [19, 24].

The output of interest often is a subset of response variables or a functional of the primary output, e.g., the integrated aerodynamic forces on a wing. Less often, SA methods are used to examine the spatially-varying influence of parameters, such as how a response field, e.g., the near-ground sound pressure level in an open field, is affected by parameter variations. We refer to this as *full-field sensitivity analysis* (FFSA). In the SA method described herein, we compute sensitivities throughout both the parameter space and the spatial grid in which the response field is simulated; hence, we call this *global, full-field sensitivity analysis*, or global FFSA.

1.3 Applying sensitivity analysis to computational mechanics models

Dosso, et al. [4] recently commented on the difficulty of making the leap from local to global sensitivity measures, but they did not use this terminology. A more complete discussion will not fit here, but we recommend considering the following points:

- Sensitivity to a parameter must be distinguished from uncertainty about that parameter's value, as sensitivity is a local characteristic of the physics model; only the analysis of sensitivity may be global. Mixing the definition of sensitivity with uncertainty confounds the interpretation of sensitivity, which exists in the physics of a specific system model, with epistemic and aleatory uncertainties, which depend on how precisely the system's properties and behavior are known. This is similar to the standard distinction in risk analysis (e.g., see Stamatelatos, et al. [22]) between a hazard and its consequences, which in our discussion are collectively analogous to sensitivity, and exposure to that hazard, which here is analogous to parameter uncertainty.
- Parameter interactions in a model will not be detected in first-order, local measures of sensitivity, which are found by changing only one parameter [24]. Scatter plots and statistics from Monte Carlo sampling (e.g., [7],[15]), principal component analysis of first-order sensitivities [24], and variance decomposition techniques [8] may highlight the effects of simultaneous parameter variations. Helton and Davis [7, p. 122] conclude that "... examination of scatter plots is always good starting point in a sensitivity study."
- When analytical derivatives are not available, local response surfaces based on standard design of experiments methods may be used to estimate sensitivities, including interaction terms [3]. This approach should be preferred over more empirical finite-differences because regression offers statistical measures of the quality of the fit, which help to assess confidence in the estimated sensitivities and to detect the presence of higher-order terms not represented in the chosen polynomial.

2 Sampling-based, full-field sensitivity analysis

In this section we present our method for global FFSA based on reduced-order models (ROMs). Sec. 2.1 outlines the method and its beneficial aspects, and Sec. 2.2 summarizes a recent application of this method to computations of the near-ground sound pressure level in a refracting atmospheric surface layer.

2.1 Framework

We combine Latin hypercube sampling (LHS) [7, 8], proper orthogonal decomposition (POD) [9, 11], and a Bayesian forecasting method to perform sampling-based SA [7, 8] throughout both the spatial domain in a computational mechanics model and a broad region of the underlying parameter space. Pettit and Wilson [15] provide some details of the method and an extensive analysis of its application to a six-parameter, near-ground sound propagation problem. In a complementary paper, Pettit and Wilson [16] offer a more complete derivation of the SA method and demonstrate a way to estimate the forecast uncertainty of the sensitivities.

LHS is used to select samples from the full range of possible parameter combinations, and the model is solved to produce the associated response fields. POD is used to condense this ensemble in terms of a small number of orthogonal basis vectors, i.e., POD modes. FFSA is done efficiently by estimating the sensitivity of each POD coefficient and combining these coefficient sensitivities into an estimate of the process's sensitivity at each spatial grid point. The Bayesian forecasting method uses cluster-weighted models (CWMs) [6] of the POD coefficients to regularize the estimation of sensitivities. A CWM is computed for each POD coefficient, and sensitivities of each CWM's conditional forecast are found through either local regression or analytical differentiation. Local regression was employed first [15], but analytical differentiation recently was shown to be much faster and more robust [16].

The payoff from using CWMs in place of the more common polynomial response surfaces is that CWMs are easily tailored to encode local nonlinear variations in the training data; in this sense, the CWMs fill the same role as neural networks often do, but CWMs have the merit of naturally providing an estimate of the conditional forecast variance (see Sec. 2.2), which gives insight into the precision of the forecasts. The CWM framework also seems to the authors to be somewhat less empirical and more transparent than common neural network architectures, and they seem to require less training to achieve satisfactory out-of-sample accuracy; however, no rigorous study was found that compares the performance of neural networks and CWMs.

Notable benefits of this SA method are summarized here: (1) it may be used with any existing computational model in a wrap-around manner, (2) it provides a built-in mechanism for estimating its own forecast uncertainties, and (3) it yields analytical sensitivities of the ROMs directly, so no approximations are made beyond those intrinsic to the ROMs based on POD and CWM.

2.2 Global, full-field sensitivities of near-ground sound pressure level

Two-dimensional fields of near-ground sound pressure level in a refracting atmosphere were computed with a wide-angle parabolic equation (PE) approximation [25, 18], which is solved with the Crank-Nicholson scheme. The 2-D domain included $0 \leqslant x \leqslant 1000$ m parallel to and $0 \leqslant z \leqslant 400$ m above the flat ground, and a 150 Hz source was placed at $x = 0.0$ m and $z = 1.0$ m above the ground. Turbulence was not included in the calculations, and the ground's acoustic impedance was represented by a relaxation model [26, 12]. The mean wind and temperature profile were represented through Monin-Obukhov similarity theory [14, 23]. For each

Table 1: Parameters in the Monin-Obukhov similarity model for wind speed and temperature profiles and the relaxation model for ground acoustic impedance.

Parameter	Symbol	Units	Values
Porosity	Ω	n/a	0.525
Flow resistivity	σ	$\mathrm{kPa \cdot s/m^2}$	$[150, 600] \times 10^3$
Surface heat flux	Q_s	$\mathrm{W/m^2}$	0
Friction velocity	u_*	m/s	0.3
Wind direction	α	deg	$[0, 180]$
Roughness length	z_0	m	0.05

LHS realization, the output was the sound pressure level (SPL) in dB (i.e., 20 times the logarithm of the complex sound pressure amplitude relative to the free-field sound pressure amplitude) at each grid point.

We [15] recently performed a preliminary SA with the six parameters listed in the first column of Table 1, but we show a restricted case here because of limited space. Only the wind direction, α, and flow resistivity, σ, were allowed to vary over the ranges described in Ref. [15]; the other parameters were fixed as listed in Table 1 to indicate typical mean conditions at mid-latitudes in open fields. $N = 250$ Latin hypercube samples was selected from the σ and α ranges. For each sample vector, the ground's acoustic impedance, and wind and temperature profiles were computed. The PE model then was solved for each parameter combination to estimate the associated sound pressure fields.

From this ensemble of $N_s = 250$ realizations, the POD modes, $\{\varphi\}_{n=1}^{N_s}$, were computed and the $N_r = 6$ strongest modes were retained for simulations throughout the parameter space. A CWM model was then found for each of the retained POD coefficients, $\{a^{(n)}\}_{n=1}^{N_r}$; e.g., Fig. 1 shows the CWM of the strongest mode, the locations of LHS samples, and the exemplar from each cluster. Realizations from additional samples, $(\sigma(\omega), \alpha(\omega))$, where ω is an element of the sample space, were then computed through a linear combination of the retained POD modes:

$$p(\sigma(\omega), \alpha(\omega)) = \sum_{n=1}^{N_r} \varphi_n a^{(n)}(\sigma(\omega), \alpha(\omega)). \tag{1}$$

Because each CWM, $f(a^{(n)}, \zeta')$, is actually an *a posteriori* estimate of a POD coefficient's probability density function throughout the sampled $\zeta = (\sigma, \alpha)$ range, the CWM forecast of each $a^{(n)}$ for a given $\zeta = \zeta'$ is the conditional expectation,

$$\left\langle a^{(n)} | \zeta' \right\rangle = \int a^{(n)} f(a^{(n)}, \zeta')\, da^{(n)} \tag{2}$$

and the forecast uncertainty is estimated with the square-root of the conditional variance,

$$\left\langle \sigma^2_{a^{(n)}} | \zeta' \right\rangle = \int \left(a^{(n)} - \left\langle a^{(n)} | \zeta' \right\rangle \right)^2 f(a^{(n)}, \zeta')\, da^{(n)}. \tag{3}$$

Fig. 2 shows the ensemble mean of the SPL forecast uncertainty, which was computed through a simple additive error model, i.e., by replacing each $a^{(n)}$ in Eq. 1

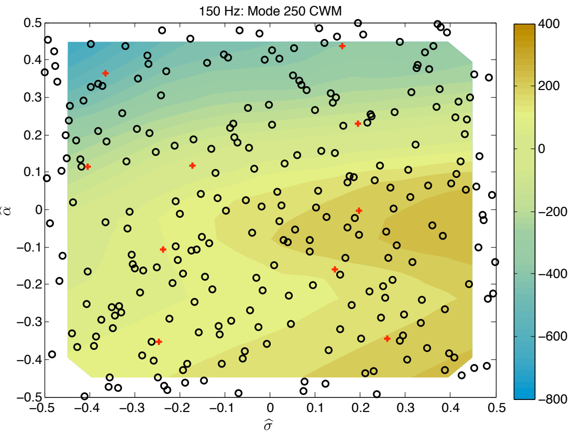

Figure 1: Cluster-weighted model of the strongest SPL mode obtained through proper-orthogonal decomposition. Normalized flow resistivity, $\hat{\sigma}$, and wind direction, $\hat{\alpha}$, are the independent variables. Black circles are parameter values from the Latin hypercube training samples. Red plus symbols are the final location each cluster's mean parameter vector.

with $\left\langle \sigma^2_{a^{(n)}} | \zeta' \right\rangle^{\frac{1}{2}}$. Although each $\left\langle \sigma^2_{a^{(n)}} | \zeta' \right\rangle^{\frac{1}{2}}$ is by definition positive, the SPL forecast uncertainty can be negative in parts of the spatial domain because the POD modes may contain negative values. Pettit and Wilson [16] show plots of the modes used here.

An ensemble of 100 full-field SPL sensitivity forecasts, S^p_σ and S^p_α, were computed to allow examination of the associated sample statistics. The absolute value of the sensitivity of each realization was used to compute the mean sensitivity because S^p_α was found to depend greatly on whether a given realization featured upwind ($90\,\mathrm{deg} \leqslant \alpha \leqslant 180\,\mathrm{deg}$) or downwind ($0\,\mathrm{deg} \leqslant \alpha < 90\,\mathrm{deg}$) conditions. Fig. 3 shows that mostly negative values of S^p_α were found for upwind conditions and primarily positive values were found downwind conditions. Consequently, when these forecast sensitivity realizations were averaged democratically, the mean values misleadingly small. This gave the impression that SPL depended little on the wind direction, which empirically is false. Using the absolute value of the sensitivity forecast provides a more realistic picture of the importance of wind direction. $|S^p_\alpha|$ was found to be greater than $|S^p_\sigma|$ throughout most of the spatial domain, especially in upwind conditions. They are most comparable near the ground in downwind conditions.

Fig. 4 shows the ensemble mean value of the forecast uncertainty, i.e., the conditional standard deviation, in the 100 SPL sensitivity realizations. Uncertainty in the forecast of the SPL sensitivity both to static flow resistivity and wind direction is greatest near the ground and at downrange locations because these locations also exhibit the greatest variation in sensitivity; see Pettit and Wilson [16] for more details.

3 Conclusions

Global sensitivity analysis of complex models is facilitated through efficient reduced-order models. Latin hypercube sampling and proper orthogonal decomposition

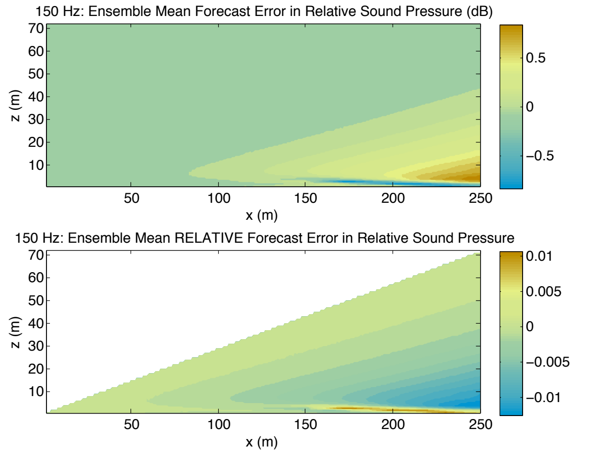

Figure 2: (Top) Ensemble mean forecast uncertainty in the sound pressure level (SPL) expressed in decibels. This plot is based on a new Latin hypercube sample of 100 realizations. (Bottom) Same as top frame but scaled at each spatial location by the corresponding ensemble mean SPL of the original set of 250 realizations to estimate the relative uncertainty.

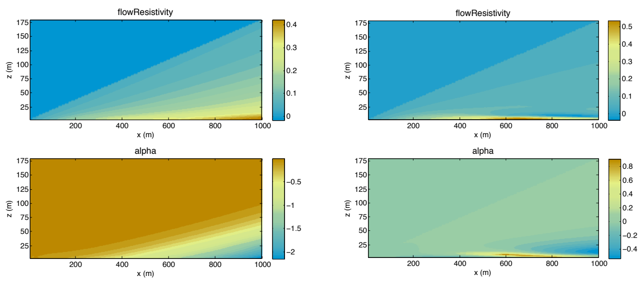

(a) Upwind

(b) Downwind

Figure 3: Ensemble average of the full-field SPL sensitivities for a 150 Hz source, but conditioned on upwind (90 deg $\leqslant \alpha \leqslant$ 180 deg) and downwind (0 deg $\leqslant \alpha <$ 90 deg) realizations.

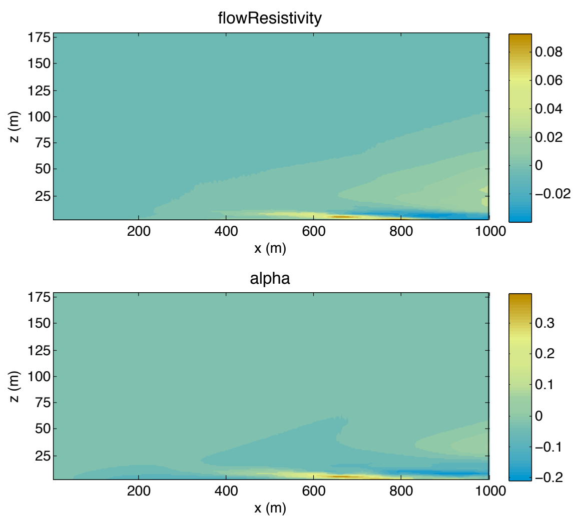

Figure 4: Ensemble mean values of the forecast uncertainty in the 100 SPL sensitivity realizations: (top) uncertainty in S^p_σ; (bottom) uncertainty in S^p_α.

were employed, in conjunction with cluster-weighted models of the POD coefficients, to simulate response fields and their sensitivities to governing parameters. POD was essential to reducing the dimensionality of the discretized response in a standard near-ground sound propagation example application.

Our method produces global, full-field sensitivities. An apparently unique result is an estimate of the sensitivity uncertainty, which helps to assess the credibility of forecast sensitivities in insufficiently-sampled regions of the parameter space, and also might be useful in assessing the ability of a grid to adequately resolve localized features in a probabilistic computational mechanics model. Pettit and Wilson [16] itemized several factors that can affect the forecasts as well as their uncertainties. These factors define the necessary components from which the ROMs are assembled, so analyzing the sensitivity of the forecasts to these choices may be viewed as a broader form of global sensitivity analysis than we have performed here; Insua, et al. [10] thoroughly explore this perspective.

In the near-ground sound propagation application, ensemble statistics of the sound pressure level sensitivities depended strongly on whether upwind or downwind propagation conditions prevailed. A related potential pitfall in sampling-based sensitivity analysis is the existence of voids in an ensemble due to sparse sampling of the parameter space. These voids can produce inconsistencies between model training and testing ensembles, and thereby complicate comparisons. They also can compromise assessments of parameter interactions.

Extreme values of a sensitivity at each grid point may be roughly estimated from the associated sample statistics. Relative values of the estimated extreme sensitivities suggest that uncertainty about both of the parameters considered here should be included in an uncertainty model if randomness, measurement imprecision, or both are expected to affect the parameters. The consequences of randomness and measurement imprecision depend too much on the details of a model to permit further generality here, but full-field sensitivity contour plots like those presented above should help to guide future studies.

The robustness and utility of any global FFSA method depend on sampling the full range of parameter variations. Latin hypercube sampling was expedient in meeting this objective, but perhaps would be surpassed by more recently developed approaches, e.g., latinized centroidal Voronoi tesselation [17]. However, the most effective use of the forecast uncertainty estimate might be in conjunction with an incremental sampling method, the goal being to run more simulations only in those regions of the parameter space that produce high forecast uncertainties. More work is needed to determine the practical utility of implementing these changes.

Parameters were represented here as independent random variables. The payoff from modeling them as random fields, e.g., with a specified level of spatial correlation, would depend on whether the physics of the system model are sensitive to this correlation. Scatter plots like those shown elsewhere by the authors [15, 16] should support this assessment, but the analyst's physical insight should be at least as important.

Acknowledgments

The first author was supported in part by a Military Interdepartmental Purchase Request from the U.S. Army Engineer Research and Development Center, Cold Regions Research and Engineering Laboratory.

References

[1] Guide for the verification and validation of computational fluid dynamics simulations. Technical Report AIAA G-077-1998, American Institute of Aeronautics and Astronautics, 1998.

[2] Y. Ben-Haim. *Info-Gap Decision Theory: Decisions Under Severe Uncertainty.* Academic Press, 2nd edition, 2006.

[3] F. Campolongo and A. Saltelli. Design of experiments. In Saltelli et al. [20], chapter 3.

[4] S. E. Dosso, P. M. Giles, G. H. Brooke, D. F. McCammon, S. Pecknold, and P. C. Hines. Linear and nonlinear measures of ocean acoustic environmental sensitivity (l). *Journal of the Acoustical Society of America*, 121(1):42–45, Jan 2007.

[5] T. F. W. Embleton. Tutorial on sound propagation outdoors. *Journal of the Acoustical Society of America*, 100(1):31–48, July 1996.

[6] N. A. Gershenfeld, B. Schoner, and E. Metois. Cluster-weighted modeling for time series prediction and characterization. *Nature*, 397:329–332, 1999.

[7] J. C. Helton and F. J. Davis. Sampling-based methods. In Saltelli et al. [20], chapter 6.

[8] J. C. Helton, J. D. Johnson, C. J. Sallaberry, and C. B. Storlie. Survey of sampling-based methods for uncertainty and sensitivity analysis. *Reliability Engineering and System Safety*, 91:1175–1209, 2006.

[9] P. Holmes, J. L. Lumley, and G. Berkooz. *Turbulence, Coherent Structures, Dynamical Systems and Symmetry.* Cambridge University Press, 1996.

[10] D. R. Insua, F. Ruggeri, and J. Martin. Bayesian sensitivity analysis. In Saltelli et al. [20], chapter 10, pages 225–244.

[11] M. Kirby. *Geometric Data Analysis.* Wiley-Interscience, 2001.

[12] M. Mungiole and D. K. Wilson. Prediction of outdoor sound transmission loss with an artificial neural network. *Applied Acoustics*, 67:324–345, 2006.

[13] E. Nikolaidis, D. M. Ghiocel, and S. Singhal, editors. *Engineering Design Reliability Handbook.* CRC Press, Boca Raton, FL, 2005.

[14] H. A. Panofsky and J. A. Dutton. *Atmospheric Turbulence: Models and Methods for Engineering Applications.* Wiley & Sons, New York, 1983.

[15] C. L. Pettit and D. K. Wilson. Proper orthogonal decomposition and cluster weighted modeling for sensitivity analysis of sound propagation in the atmospheric surface layer. *Journal of the Acoustical Society of America*, 122(3):1374–1390, Sep 2007.

[16] C. L. Pettit and D. K. Wilson. Sampling-based sensitivity analysis through proper orthogonal decomposition and cluster-weighted models. In *10th AIAA Non-Deterministic Approaches Conference*, number AIAA-2008-1988, Schaumburg, IL, USA, April 2008.

[17] V. J. Romero, J. V. Burkardt, M. D. Gunzburger, and J. S. Peterson. Initial evaluation of pure and "latinized" centroidal voronoi tessellation for non-uniform statistical sampling. In *4th International Conference on Sensitivity Analysis of Model Output (SAMO'04)*, Santa Fe, NM, March 2004.

[18] E. M. Salomons. *Computational Atmospheric Acoustics.* Kluwer Academic Publishers, Dordrecht, The Netherlands, 2001.

[19] A. Saltelli. What is sensitivity analysis? In Saltelli et al. [20], chapter 1.

[20] A. Saltelli, K. Chan, and E. M. Scott, editors. *Sensitivity Analysis.* John Wiley & Sons, New York, 2000.

[21] L. E. Schwer. An overview of the ASME guide for verification and validation in computational solid mechanics. In *LS-DYNA Anwenderforum*, http://www.dynamore.de/download/af06/papers/A-II-4.pdf, 2006. DYNAmore.

[22] M. Stamatelatos, G. Apostolakis, H. Dezfuli, C. Everline, S. Guarro, P. Moieni, A. Mosleh, T. Paulos, and R. Youngbload. *Probabilistic Risk Assessment Procedures Guide for NASA Managers and Practitioners.* NASA Headquarters - Office of Safety and Mission Assurance, August 2002.

[23] R. B. Stull. *An Introduction to Boundary Layer Meteorology.* Kluwer, Dordrecht, Germany, 1998.

[24] T. Turanyi and H. Rabitz. Local methods. In Saltelli et al. [20], chapter 5.

[25] M. West, K. Gilbert, and R. A. Sack. A tutorial on the parabolic equation (PE) model used for long range sound propagation in the atmosphere. *Applied Acoustics*, 37:31–49, 1992.

[26] D. K. Wilson. Simple, relaxational models for the acoustical properties of porous media. *Applied Acoustics*, 50:171–188, 1997.

[27] D. K. Wilson, E. L. Andreas, C. L. Pettit, E. G. Patton, P. P. Sullivan, and J. W. Weatherly. Characterization of uncertainty in outdoor sound propagation predictions. *Journal of the Acoustical Society of America*, 121:EL177–EL183, 2007.